Ethanol conversion to C_{4+} olefins over bimetallic copper- and lanthanum-containing Beta zeolite catalysts

Michael J. Cordon,[a‡] Junyan Zhang,[a,b‡] Nohor "River" Samad,[c] James W. Harris,[c] Meijun Li,[d] Dongxia Liu,[b] and Zhenglong Li *[a]

[a]Manufacturing Science Division, Oak Ridge National Laboratory, Oak Ridge, TN 37830, USA.

[b]Department of Chemical and Biomolecular Engineering, University of Maryland, College Park, MD 20742, USA.

[c]Department of Chemical and Biological Engineering, The University of Alabama, Tuscaloosa, AL 35487, USA.

[d]Chemical Science Division, Oak Ridge National Laboratory, Oak Ridge, TN 37830, USA.

*Corresponding author: liz3@ornl.gov.

KEYWORDS Ethanol, lanthanum, copper, Beta zeolite, catalysis, olefins

ABSTRACT: Ethanol conversion to C_{4+} olefins remains a critical yet nonselective process for producing renewable middle distillates. Here, Cu-La/Beta catalysts comprised of copper and lanthanum incorporated onto a dealuminated Beta support are reported for ethanol conversion to C_{4+} olefins (73% selectivity, ~98% ethanol conversion, 623 K) with <4% C_1-C_3 hydrocarbons, particularly favoring C_{5+} olefin formation (43% selectivity), distinct from the benchmarking Cu-Y/Beta catalyst. Monometallic Cu/Beta or La/Beta samples are insufficient to catalyze the C_{4+} olefin formation and primarily form dehydration products (e.g., ethylene and diethyl ether), indicating the necessity of both Cu and La species for butene and C_{5+} olefin formation. Increasing the bulk La loading at a fixed Cu content yields higher C_{5+} olefins until the La/Cu molar ratio reaches 3.6. These findings indicate Cu-La/Beta as an effective ethanol conversion catalyst that facilitates multiple C-C bond formation events required for synthesizing C_{5+} olefins (i.e., hexenes and octenes).

Sustainable middle distillate fuels production from renewable sources is critical for decarbonizing transportation sectors such as aviation, marine and heavy-duty diesel applications which remain difficult to electrify. C_{4+} olefins (i.e., butenes, hexenes, and octenes) are key platform molecules for downstream oligomerization into middle-distillate-range hydrocarbons, thus renewably generating C_{4+} olefins is a key focus in many biomass-to-middle-distillate pathways.[1–5] Ethanol is a prominent renewable feedstock (~86 million tons produced worldwide in 2018[6]) that can be directly converted to C_{4+} olefins via either acetaldehyde or ethylene intermediates, the former of which leads to greater C_{4+} olefin selectivity.[7] Emerging technologies in ethanol synthesis from CO_2[8] also offer a unique opportunity to bridge CO_2 valorization to middle distillate production with ethanol as a critical intermediate, potentially leading to emission-negative approaches to decarbonize transportation.

Using acetaldehyde as the key C_2 intermediate to C_{4+} olefins, the ethanol conversion reaction network begins with ethanol dehydrogenation and subsequent aldol condensation to crotonaldehyde followed by either Meerwein-Ponndorf-Verley (MPV) reduction to crotyl alcohol[7,9] or hydrogenation to butyraldehyde[10] (Scheme S.1). Butene isomers are then formed from either the dehydration of crotyl alcohol to 1,3-butadiene and subsequent selective hydrogenation or the reduction of butyraldehyde to 1-butanol and subsequent dehydration. Both reaction networks require catalytic functionalities for (de)hydrogenation, aldol condensation, MPV reduction and dehydration reactions, each of which may require unique active site properties to increase butene selectivity. Further, competing reactions such as ethanol dehydration should be minimized to mitigate ethylene formation and associated decreases in butene selectivity. Recently, multifunctional yttrium-containing zeolite catalysts (i.e., Zn-Y/Beta combined with hydrogenation catalyst[7], Cu-Zn-Y/Beta[10]) have been shown to selectively produce butene-rich olefin streams from ethanol with low C_{5+} olefin selectivities (i.e., hexenes, octenes), indicating minimal sequential aldol condensation. Longer carbon chain (C_{5+}) olefins are

desirable feedstocks for renewable jet and diesel fuel production[4,5] as they only require dimerization to generate middle-distillate-range hydrocarbons, potentially leading to overall higher distillate yield. However, the other notable route for ethanol conversion to C_{5+} hydrocarbons in one reactor is over Brønsted acid zeolites (e.g., H-ZSM-5), which primarily generates aromatic-rich hydrocarbons[11,12].

Inspired by the ethanol to olefins reactions over the Lewis acidic Y-containing zeolite catalysts, alternative Lewis acidic heteroatoms are under investigation to replace Y which could potentially decrease the ethanol dehydration reactivity and increase the crossed aldol condensation rates of acetaldehyde with C_{4+} aldehydes (i.e., crotonaldehyde, butyraldehyde) relative to MPV reduction or hydrogenation of C_4 aldehydes. This would favor C_{4+} product formation while also effectively shifting olefin compositions towards longer (C_{5+}) olefins. One such heteroatom is La which, given its similar electronic structure to Y but slightly weaker Lewis acidity[13], could generate Lewis acid sites capable of catalyzing aldol condensation reactions. These La sites may also decrease the dehydration of C_4 alcohols (i.e., 1-butanol, crotyl alcohol) to butenes/butadiene, leading to higher concentrations of C_4 intermediates for further coupling with acetaldehyde to form C_{6+} products. La inclusion onto zeolite catalysts has nearly exclusively been investigated after ion exchange onto Al-containing zeolites (i.e., zeolite X[14], Y[15,16], Beta[17,18]). These materials are primarily used as fluid catalytic cracking (FCC) catalysts[19] with other applications including hydrocarbon alkylation[20], disproportionation of hydrogen peroxide[21], and ethanol upgrading to propylene[22].

Here, we report La-containing bimetallic zeolite catalysts (Cu-La/Beta) using a dealuminated Beta support that can directly and selectively produce C_{4+} olefins from ethanol with increased C_{5+} olefin selectivity and less ethylene formation relative to Y-containing Lewis acid zeolites. The Lewis and Brønsted acidities of metal-containing dealuminated Beta catalysts (Cu/Beta, La/Beta, and Cu-La/Beta) were probed via pyridine titration and subsequent Fourier transform transmission infrared (FTIR) spectra collection. Product distributions were measured at near complete ethanol conversions to investigate the catalytic functionalities of Cu-La/Beta for ethanol upgrading to butene, hexene, and octene isomers. These results highlight Cu-La/Beta as a promising ethanol conversion catalyst capable of facilitating the multiple C-C bond formation events required for C_{5+} olefin production from ethanol.

Monometallic Cu/Beta and La/Beta and bimetallic Cu-La/Beta zeolites were synthesized via solid state grinding of $Cu(NO_3)_2{\bullet}3H_2O$ and $La(NO_3)_3{\bullet}6H_2O$ precursors onto a dealuminated Beta support (deAl-Beta, Si/Al ratio 12.5 prior to dealumination, see Supporting Information for additional details). X-ray diffraction (XRD) patterns and micropore volumes from N_2 adsorption isotherms (77 K) are consistent with the Beta topology (Figure S.1 and S.2), although micropore volumes tend to decrease at high metal loadings. Amorphous SiO_2 features are not observed in the XRD patterns, suggesting that the decrease in micropore volumes at increased bulk metal loadings may indicate partial pore blockage by some metal species. Peaks reflective of large CuO_x or LaO_x nanoparticles are not observed in the XRD patterns. Cu, La, Si, and Al loadings were measured using inductively coupled plasma atomic emission spectroscopy (ICP-AES) with undetectable Al concentrations (Si/Al>1300) in the dealuminated Beta support and subsequent synthesized samples. Therefore, these La species are not ion exchanged onto framework Al sites within the zeolite and are distinct active sites from those present within most La-containing zeolite studies[20,23]. Cu loadings are similar on monometallic Cu/Beta and bimetallic Cu-La/Beta samples (0.9-1.0 wt%) while La loadings range from 1.0 to 12 wt% (Table S.1). These samples are denoted as Cu_x/Beta, La_y/Beta and Cu_xLa_y/Beta where x and y indicate the Cu and La weight percentages, respectively.

The Lewis and Brønsted acidities of the Cu and La species generated upon addition to deAl-Beta were investigated using transmission IR spectra collected after pyridine adsorption (423 K). Figure 1 displays transmission IR spectra collected on Cu-La/Beta, La/Beta, Cu/Beta, and deAl-Beta samples after saturation with pyridine and purging in flowing He. The spectrum collected on Cu_1/Beta shows two peaks centered at 1450 cm^{-1} and 1607 cm^{-1} while the spectrum on La_7/Beta show two peaks centered at 1444 cm^{-1} and 1600 cm^{-1}. These peaks together with an additional peak centered at ~1491 cm^{-1} reflect perturbed pyridine deformation modes that result from pyridine adsorption onto Lewis acid sites. As no prominent peaks are observed on the deAl-Beta sample after an identical saturation and purge procedure, the presence of these pyridine deformation modes reflects pyridine adsorbed onto Lewis acidic Cu or La species, respectively. Spectra collected on three Cu-La/Beta samples contain all five peaks (1444, 1450, 1491, 1600, and 1607 cm^{-1}) as expected for bimetallic compositions. Due to the lack of available integrated molar extinction coefficients for pyridine adsorbed onto Cu and La sites within zeolites, quantification of Lewis acidic Cu and La site densities is not currently possible. Notably, there are no observable peaks centered at 1545 cm^{-1} or 1637 cm^{-1} over La_7/Beta or the bimetallic samples which would reflect protonated pyridine species resulting from pyridine adsorption onto Brønsted acid sites. This indicates a lack of detectable Brønsted acid sites on the samples studied here even at high La loadings (12 wt%) on Cu_1La_{12}/Beta and is distinctive from previous observations on Y-containing Beta catalysts possessing both Lewis and Brønsted acid Y sites.[7]

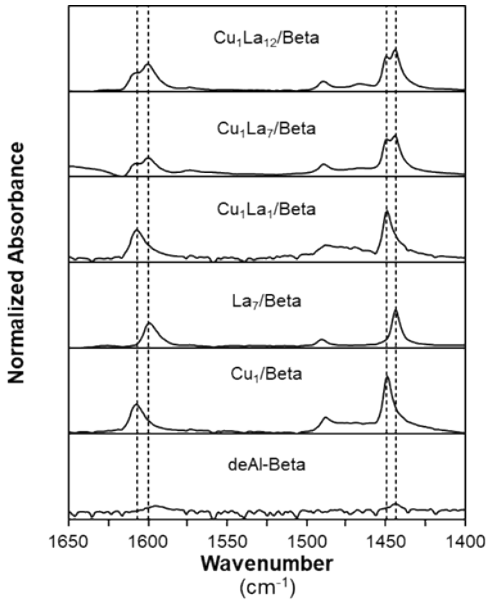

Figure 1. Transmission IR spectra of deAl-Beta, Cu_1/Beta, La_7/Beta, Cu_1La_1/Beta, Cu_1La_7/Beta, and Cu_1La_{12}/Beta samples collected after pyridine saturation at 423 K. Dashed lines are used to guide the eye.

The roles of Cu and La sites in ethanol upgrading were probed over deAl-Beta and various mono- and bimetallic Beta samples. Figure 2 depicts pseudo steady-state product distributions over deAl-Beta, Cu_1/Beta, La_7/Beta, and Cu_1La_7/Beta materials at high ethanol conversion to investigate changes in product yields caused by Cu and/or La incorporation (6.8 kPa ethanol, 623 K, 0.51 h^{-1}, product selectivities shown in Figure S.3). Ethylene is formed at high yields (~98%, 623 K) via ethanol dehydration over the metal-free deAl-Beta support and presumably reflects ethanol interactions with silanol moieties on zeolite surfaces as previously observed to 593 K over deAl-Beta[24]. The addition of Cu onto the dealuminated Beta support results in acetaldehyde formation from ethanol dehydrogenation alongside ethylene and ethane yields reflecting dehydration and subsequent hydrogenation[10,25]. Low butene yields (~6%) indicate observable C-C bond formation reactivity, presumably from ethanol dehydrogenation over Cu sites and subsequent aldol condensation. The incorporation of La sites onto deAl-Beta decreases the ethanol conversion relative to the equivalent measurement over deAl-Beta (59% vs. ~100%, 623 K) and lowers the combined yield of dehydration products (ethylene and diethyl ether, 52% and 99% over La_7/Beta and deAl-Beta, respectively, at 623 K) at a consistent space velocity, suggesting the suppression and/or elimination of some ethanol dehydration sites (see Figure S.4 for spectra of IR OH stretching region). Additionally, La_7/Beta does not provide significant reactivity for ethanol dehydrogenation at these conditions despite the relatively high La loading.

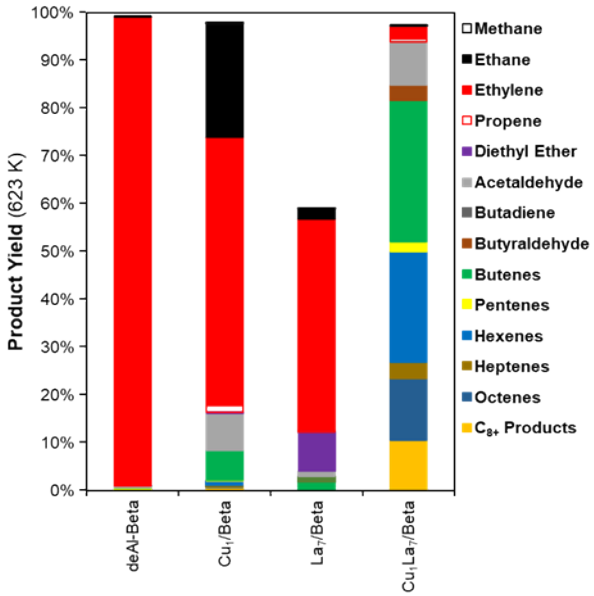

Figure 2. Steady-state ethanol upgrading product yields over deAl-Beta, Cu_1/Beta, La_7/Beta, and Cu_1La_7/Beta catalysts (6.8 kPa ethanol in 99 kPa H_2, 623 K, 0.51 h^{-1} weight hourly space velocity (WHSV)). Residual product distribution percentages reflect remaining ethanol at sub-100% conversion. Errors in product distributions are 15% under these conditions. The C_{8+} products group include C_{8+} aldehydes, C_{8+} alcohols, and C_{9+} olefins, all of which reflect sequential aldol condensation events.

The product distribution observed over bimetallic Cu_1La_7/Beta, a catalyst containing Cu and La loadings equivalent to the monometallic catalysts (Table S.1), shows a much higher selectivity towards C_{4+} olefin (73%, Figure S.3) relative to the other catalysts. As this behavior is quite distinct from either monometallic catalyst, the inclusion of both Cu and La sites onto the deAl-Beta support catalyzes one or more C-C coupling reactions and the associated reactions ultimately yielding butenes and longer olefins. While this data set does not indicate the precise pathway and associated intermediates for the formation of longer-chain olefins, several pathways involving acetaldehyde formation and subsequent aldol condensation have been observed over other multifunctional catalysts comprised of Lewis acidic and metallic species. For example, ethanol upgrading to butadiene and/or butene over Ag-ZrO_2/SiO_2 begins with dehydrogenation to acetaldehyde followed by aldol condensation to form crotonaldehyde, MPV reduction to crotyl alcohol, dehydration to butadiene,[9] and finally hydrogenation to butene isomers. A similar reaction pathway was also suggested over a composite catalyst of Zn-Y/Beta and single-atom alloy Pt-Cu/Al_2O_3.[7] An alternative pathway was observed over Cu-Zn-Y/Beta that follows similar steps to form crotonaldehyde but then diverges by directly hydrogenating crotonaldehyde to butyraldehyde prior to butene formation[10]. Regardless of the exact reaction pathway, the observed decrease in ethylene formation over monometallic La_7/Beta or Cu_1/Beta and the concomitant increase in acetaldehyde formation over Cu_1/Beta suggests that Cu_1La_7/Beta catalyzes a similar acetaldehyde-mediated pathway as Ag-

ZrO_2/SiO_2 or Cu-Zn-Y/Beta rather than one based on ethanol dehydration to ethylene and subsequent oligomerization to longer olefins. Indeed, limited C_{4+} olefin formation over either Cu_1/Beta or La_7/Beta despite sufficient ethylene partial pressures indicates that C-C bond formation reactions do not reflect ethylene oligomerization over Cu or La sites.

Based on these observations, Scheme 1 depicts a potential reaction network capable of facilitating C_4-C_6 olefin formation using acetaldehyde as the key C_2 building block (see Scheme S.2 for an expanded reaction network for C_8 formation). Upon acetaldehyde aldol condensation, crotonaldehyde can be hydrogenated to butyraldehyde, reduced via MPV reduction to crotyl alcohol, or condensed with an additional acetaldehyde to form a C_6 aldehyde. The relative rates of these competing reactions impact the product distributions and the associated C_4:C_{6+} olefin ratio. Once alcohol groups are formed on C_{4+} compounds, the formation of mono-olefin compounds occurs via sequential hydrogenation and dehydration or vice versa. Further carbon chain growth occurs via crossed aldol condensation reactions between acetaldehyde and either C_4 aldehydes (i.e., butyraldehyde, crotonaldehyde) or C_6 aldehydes. These C_6 and C_8 aldehydes can then undergo similar MPV reduction, hydrogenation, and dehydration reactions to those forming butene isomers from C_4 aldehydes. Taken together, this generalized reaction network represents the wide range of potential reactions capable of generating the products observed over Cu_1La_7/Beta with C_4-C_8 olefins as the primary products. Scheme 1 denotes only the linear unsaturated intermediates/products for clarity, yet a range of isomers can be generated for C_6 and C_8 compounds due to branching during aldol condensation events. We also note that some of the observed octene formation could reflect aldol condensation reactions between C_4 aldehydes which would likely result in branched aldehydes and subsequent olefin compounds. Further, the observation of C_5 and C_7 olefins may suggest additional aldol condensation reactions between acetaldehyde or C_4 aldehydes and acetone as has previously been suggested on Ag-ZrO_2/SiO_2.[9]

Scheme 1. Proposed reaction network for ethanol upgrading to butene, hexene, and octene isomers over Cu-La/Beta. Additional schemes are readily generated to incorporate further aldol condensation events and associated dehydration and hydrogenation reactions. Compounds within parentheses may exist as multiple isomers. Direct coupling of ethanol (or C_{4+} alcohols) with aldehydes is possible, which is not included in this reaction network. The [H_2] designation indicates either alcohols or molecular hydrogen as hydrogen donors.

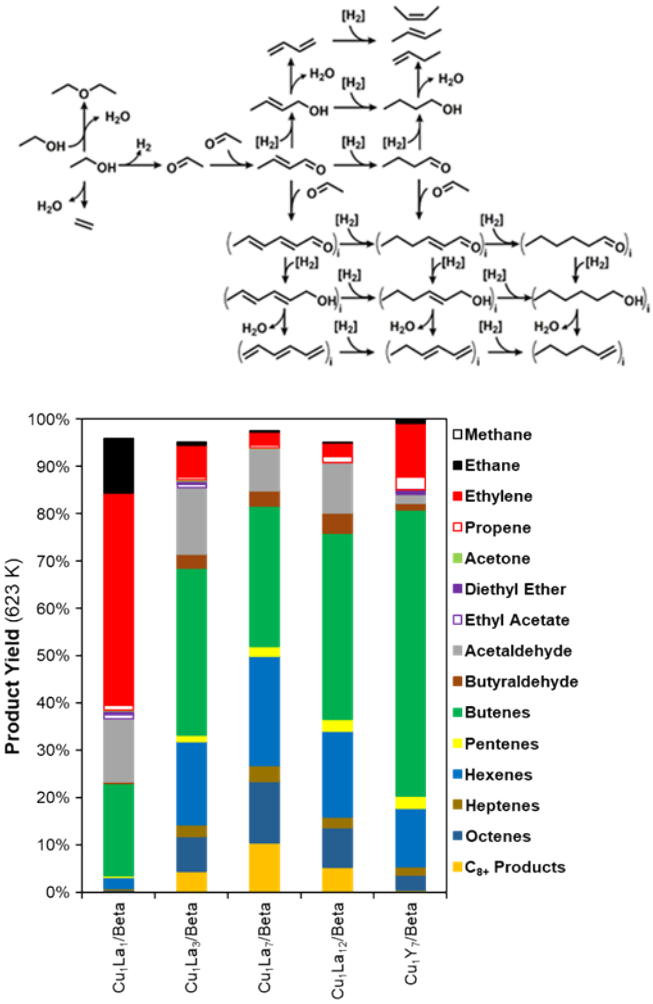

Figure 3. Steady-state ethanol upgrading product yields obtained over Cu-La/Beta catalysts as a function of La loading and over Cu_1Y_7/Beta (6.8 kPa ethanol in 99 kPa H_2, 623 K, WHSV = 0.51 h^{-1}). Residual product distribution percentages reflect remaining ethanol at sub-100% conversion. Errors in product distributions are 15% under these conditions. The C_{8+} products group include C_{8+} aldehydes, C_{8+} alcohols, and C_{9+} olefins, all of which reflect sequential aldol condensation events.

Since the Y Lewis acid site density has been linked to aldol condensation reactivity on Cu-Zn-Y/Beta[10] and Zn-Y/Beta,[26] the concentration of La sites was varied to alter the aldol condensation reactivity per gram of catalyst and the associated olefin product distribution. Figure 3 shows product distributions obtained over bimetallic Cu-La/Beta catalysts as a function of La loading (6.8 kPa ethanol in 99 kPa H_2, 623 K, WHSV = 0.51 h^{-1}, >95% conversion). Product distributions are composed of a mix of butene, hexene, and octene isomers with lower yields towards pentenes and heptenes, oxygenates (diethyl ether, ethyl acetate, acetaldehyde, acetone, 1-butanol), and short-chain hydrocarbons (predominantly ethylene and ethane with trace methane and propene), and a small yield of unidentified C_{8+} products at high La loadings (product selectivities shown in Figure S.5). The product distributions shown here average multiple pseudo steady state product distributions collected over each catalyst (<5% difference

between subsequent GC injections). Figure S.6 in the Supporting Information depicts a representative plot of ethanol conversion and individual product yield as a function of time on stream over Cu_1La_{12}/Beta.

The product distribution observed over Cu_1La_1/Beta is similar to Cu_1/Beta but with decreased ethane and ethylene formation and concomitant increases in acetaldehyde and butene yields; however, significant yields of C_{5+} olefins are absent, suggesting the need for additional La sites for sufficient aldol condensation reactivity (per gram of catalyst). Increasing the La loading to a nearly stoichiometric Cu and La molar ratio on Cu_1La_3/Beta (La/Cu = 1.3, Table S.1) shifts the product distribution towards C_{4+} products (primarily C_{4+} olefins) and reduces C_1-C_3 paraffins and C_2-C_3 olefin yields, indicating increased aldol condensation activity towards C-C coupling products. The relative ratio of C_{5+}/C_4 product yields, reflecting the competition between further crossed aldol condensation of acetaldehyde and a C_4 aldehyde and the cascading hydrogenation/dehydration reactions of C_4 aldehydes to butenes, increases dramatically from 0.2 to 1.0 as the La loading changes from 1.0 to 3.0 wt% (Figure S.7 and Table S.1). Further increasing the La loading to La/Cu = 3.6 on Cu_1La_7/Beta leads to higher C_{5+} product yields (from 33% to 52% over Cu_1La_3/Beta and Cu_1La_7/Beta, respectively, Figure 3) with a concomitant reduction in butene yield, which is further reflected in a higher C_{5+}/C_4 product ratio (1.8, Figure S.7). As variations in ethylene or other side product yields are negligible at higher La loadings, increased C_{5+} product formation reflects multiple C-C coupling events likely between C_{4+} aldehydes and acetaldehyde. Further increasing the La loading to 12 wt% (La/Cu = 6.6) does not further increase the C_{5+} product yield, suggesting an optimal Cu:La molar ratio between 1.3 and 6.6 for longer chain product formation at these reaction conditions.

Notably, the steady-state product distribution observed over Cu_1La_7/Beta indicates a combined C_4-C_8 olefin selectivity of 73% (87% overall C_{4+} products, 98% conversion, Figure S.5). This contrasts the product distribution observed over Cu_1Y_7/Beta (Figure S.5) comprised of 61% butenes and 20% C_{5+} olefins selectivities (C_{5+}/C_4 product ratio of 0.3, Figure S.7), suggesting an increased aldol condensation reactivity of acetaldehyde with C_{4+} aldehydes over La sites, a decreased reactivity for C_4 aldehyde hydrogenation (i.e., differences in Cu species), and/or a decreased C_4 alcohol dehydration over Cu-La/Beta catalysts. Further, Cu_1La_7/Beta produces much less ethylene than Cu_1Y_7/Beta (2.8% selectivity over Cu_1La_7/Beta vs 11% over Cu_1Y_7/Beta, Figure S.5), potentially due to the absence of La Brønsted acid sites (Figure 1) or weaker Lewis acidity of La relative to Y[13]. Ethylene is an undesired product for middle distillates production as it cannot be further converted to longer-chain products under these reaction conditions or typical C_{4+} olefins oligomerization conditions[27]. Both acetaldehyde and butyraldehyde could be recycled to further improve targeted C_{4+} olefin selectivity. Altogether, Cu-La/Beta is shown to be a relevant and selective catalyst for ethanol conversion to C_{4+} products for the purpose of producing middle distillates. Further investigations of the Cu and La active sites and the associated reaction mechanism(s) leading to the higher C_{5+} olefins selectivity relative to other ethanol conversion catalysts will be conducted in future studies.

Conclusions

In summary, thermocatalytic ethanol conversion remains a critical pathway for generating renewable olefins as precursors to fuels and commodity chemicals production. Cu- and La-containing Beta zeolites were investigated for ethanol-to-olefins production by combining the ethanol dehydrogenation reactivity of Cu sites with La sites that catalyze C-C coupling reactions. This bimetallic Cu-La formulation mitigates ethylene formation over the deAl-Beta support while yielding C_{4+} olefins including significant C_{5+} products (73% C_{4+} olefin selectivity, 43% C_{5+} olefin selectivity, ~98% ethanol conversion), indicating that both single and sequential C-C coupling events occur to form longer chain products. This behavior is not observed over the monometallic Cu_1/Beta or La_7/Beta catalysts, and the associated product distributions are significantly affected by varying the La loading within a 0.4-6.6 Cu:La molar ratio range. The production of C_{4+} olefins with a significant C_{5+} olefins yield over bimetallic Cu-La/Beta catalysts is a promising step towards the production of renewable middle distillate fuels. Future investigations will focus on active site quantification and identifying the confining environment's effects on reaction rates and selectivities towards longer chain olefin compounds.

ASSOCIATED CONTENT

Supporting Information. The following files are available free of charge: experimental methods, additional reaction schemes, bulk characterization data, additional product distribution plots. This material is available free of charge via the Internet at http://pubs.acs.org.

AUTHOR INFORMATION

Corresponding Author

* liz3@ornl.gov

Author Contributions

The manuscript was written through contributions of all authors. All authors have given approval to the final version of the manuscript. ‡These authors contributed equally.

Funding Sources

Funding provided by the U.S. Department of Energy, Office of Energy Efficiency and Renewable Energy (EERE), Bioenergy Technologies Office (BETO), under contract DE-AC05-00OR22725 (ORNL) with UT-Battle, LLC, and in collaboration with the Chemical Catalysis for Bioenergy (ChemCatBio) Consortium, a member of the Energy Materials Network. Z.L. also acknowledge funding from the Center for Bioenergy Innovation, a U.S. DOE Bioenergy Research Center supported by the Office of Biological and Environmental Research in the DOE Office of Science and led by Oak Ridge National Laboratory. X-ray data measurements and analyses were partly conducted at the Center for Nanophase Materials Sciences (CNMS), which is a DOE Office of Science User

Facility. We acknowledge Dr. Jong Keum's help in XRD data measurements. The views and opinions of the authors expressed herein do not necessarily state or reflect those of the United States Government or any agency thereof. Neither the United States Government nor any agency thereof, nor any of their employees, makes any warranty, expressed or implied, or assumes any legal liability or responsibility for the accuracy, completeness, or usefulness of any information, apparatus, product, or process disclosed, or represents that its use would not infringe privately owned rights.

Conflict of Interest Statement

A United States patent application is pending for the inventors J.Z. and Z. L.

REFERENCES

(1) Adhikari, S. P.; Zhang, J.; Guo, Q.; Unocic, K. A.; Tao, L.; Li, Z. A Hybrid Pathway to Biojet Fuel via 2,3-Butanediol. *Sustain. Energy Fuels* **2020**, *4* (8), 3904–3914. https://doi.org/10.1039/d0se00480d.

(2) Eagan, N. M.; Kumbhalkar, M. D.; Buchanan, J. S.; Dumesic, J. A.; Huber, G. W. Chemistries and Processes for the Conversion of Ethanol into Middle-Distillate Fuels. *Nat. Rev. Chem.* **2019**, *3* (4), 223–249. https://doi.org/10.1038/s41570-019-0084-4.

(3) Bond, J. Q.; Alonso, D. M.; Wang, D.; West, R. M.; Dumesic, J. A. Integrated Catalytic Conversion of Gamma-Valerolactone to Liquid Alkenes for Transportation Fuels. *Science (80-.).* **2010**, *327* (5969), 1110–1114. https://doi.org/10.1126/science.1184362.

(4) Harvey, B. G.; Meylemans, H. A. 1-Hexene: A Renewable C6 Platform for Full-Performance Jet and Diesel Fuels. *Green Chem.* **2014**, *16* (2), 770–776. https://doi.org/10.1039/c3gc41554f.

(5) Harvey, B. G.; Quintana, R. L. Synthesis of Renewable Jet and Diesel Fuels from 2-Ethyl-1-Hexene. *Energy Environ. Sci.* **2010**, *3* (3), 352–357. https://doi.org/10.1039/b924004g.

(6) Renewable Fuels Association. *2019 Ethanol Industry Outlook*; 2019.

(7) Cordon, M. J.; Zhang, J.; Purdy, S. C.; Wegener, E. C.; Unocic, K. A.; Allard, L. F.; Zhou, M.; Assary, R. S.; Miller, J. T.; Krause, T. R.; et al. Selective Butene Formation in Direct Ethanol-to-C3+-Olefin Valorization over Zn–Y/Beta and Single-Atom Alloy Composite Catalysts Using In Situ-Generated Hydrogen. *ACS Catal.* **2021**, *11* (12), 7193–7209. https://doi.org/10.1021/acscatal.1c01136.

(8) Li, F.; Li, Y. C.; Wang, Z.; Li, J.; Nam, D.-H.; Lum, Y.; Luo, M.; Wang, X.; Ozden, A.; Hung, S.-F.; et al. Cooperative CO2-to-Ethanol Conversion via Enriched Intermediates at Molecule-Metal Catalyst Interfaces. *Nat. Catal.* **2020**, *3* (1), 75–82. https://doi.org/10.1038/s41929-019-0383-7.

(9) Dagle, V. L.; Winkelman, A. D.; Jaegers, N. R.; Saavedra-Lopez, J.; Hu, J.; Engelhard, M. H.; Habas, S. E.; Akhade, S. A.; Kovarik, L.; Glezakou, V.-A.; et al. Single-Step Conversion of Ethanol to n-Butene over Ag-ZrO2/SiO2 Catalysts. *ACS Catal.* **2020**, *10* (18), 10602–10613. https://doi.org/10.1021/acscatal.0c02235.

(10) Zhang, J.; Wegener, E. C.; Samad, N. R.; Harris, J. W.; Unocic, K. A.; Allard, L. F.; Purdy, S.; Adhikari, S.; Cordon, M. J.; Miller, J. T.; et al. Isolated Metal Sites in Cu–Zn–Y/Beta for Direct and Selective Butene-Rich C3+ Olefin Formation from Ethanol. *ACS Catal.* **2021**, *11* (15), 9885–9897. https://doi.org/10.1021/acscatal.1c02177.

(11) Chowdhury, A. D.; Paioni, A. L.; Whiting, G. T.; Fu, D. L.; Baldus, M.; Weckhuysen, B. M. Unraveling the Homologation Reaction Sequence of the Zeolite-Catalyzed Ethanol-to-Hydrocarbons Process. *Angew. Chemie-International Ed.* **2019**, *58* (12), 3908–3912. https://doi.org/10.1002/anie.201814268.

(12) Li, Z. L.; Lepore, A. W.; Salazar, M. F.; Foo, G. S.; Davison, B. H.; Wu, Z. L.; Narula, C. K. Selective Conversion of Bio-Derived Ethanol to Renewable BTX over Ga-ZSM-5. *Green Chem.* **2017**, *19* (18), 4344–4352. https://doi.org/10.1039/c7gc01188a.

(13) Tsuruta, H.; Yamaguchi, K.; Imamoto, T. Tandem Mass Spectrometric Analysis of Rare Earth(III) Complexes: Evaluation of the Relative Strength of Their Lewis Acidity. *Tetrahedron* **2003**, *59* (52), 10419–10438. https://doi.org/10.1016/j.tet.2003.06.006.

(14) Schussler, F.; Pidko, E. A.; Kolvenbach, R.; Sievers, C.; Hensen, E. J. M.; van Santen, R. A.; Lercher, J. A. Nature and Location of Cationic Lanthanum Species in High Alumina Containing Faujasite Type Zeolites. *J. Phys. Chem. C* **2011**, *115* (44), 21763–21776. https://doi.org/10.1021/jp205771e.

(15) Smith, J. V; Bennett, J. M.; Flanigen, E. M. Dehydrated Lanthanum-Exchanged Type Y Zeolite. *Nature* **1967**, *215* (5098), 241-. https://doi.org/10.1038/215241a0.

(16) Huang, J.; Jiang, Y.; Marthala, V. R.; Ooi, Y. S.; Weitkarnp, J.; Hunger, M. Concentration and Acid Strength of Hydroxyl Groups in Zeolites La,Na-X and La,Na-Y with Different Lanthanum Exchange Degrees Studied by Solid-State NMR Spectroscopy. *Microporous Mesoporous Mater.* **2007**, *104* (1–3), 129–136. https://doi.org/10.1016/j.micromeso.2007.01.016.

(17) Jia, C. J.; Beaunier, P.; Massiani, P. Comparison of Conventional and Solid-State Ion Exchange Procedures for the Incorporation of Lanthanum in H-Beta Zeolite. *Microporous Mesoporous Mater.* **1998**, *24* (1–3), 69–82. https://doi.org/10.1016/S1387-1811(98)00144-9.

(18) Gaare, K.; Akporiaye, D. Modified Zeolites as Catalysts in the Friedel-Crafts Acylation. *J. Mol. Catal. A-Chemical* **1996**, *109* (2), 177–187. https://doi.org/10.1016/1381-1169(96)00023-4.

(19) Louwen, J. N.; Simko, S.; Stanciakova, K.; Bulo, R. E.; Weckhuysen, B. M.; Vogt, E. T. C. Role of Rare Earth Ions in the Prevention of Dealumination of Zeolite Y for Fluid Cracking Catalysts. *J. Phys. Chem. C* **2020**, *124* (8), 4626–4636. https://doi.org/10.1021/acs.jpcc.9b11956.

(20) Guzman, A.; Zuazo, I.; Feller, A.; Olindo, R.; Sievers, C.; Lercher, J. A. On the Formation of the Acid Sites in Lanthanum Exchanged X Zeolites Used for Isobutane/Cis-2-Butene Alkylation. *Microporous Mesoporous Mater.* **2005**, *83* (1–3), 309–318. https://doi.org/10.1016/j.micromeso.2005.04.024.

(21) Wahlen, J.; De Hertogh, S.; De Vos, D. E.; Nardello, W.; Bogaert, S.; Aubry, J. M.; Alsters, P. L.; Jacobs, P. A. Disproportionation of Hydrogen Peroxide into Singlet Oxygen Catalyzed by Lanthanum-Exchanged Zeolites. *J. Catal.* **2005**, *233* (2), 422–433. https://doi.org/10.1016/j.jcat.2005.05.013.

(22) Furumoto, Y.; Tsunoji, N.; Ide, Y.; Sadakane, M.; Sano, T. Conversion of Ethanol to Propylene over HZSM-5(Ga) Co-Modified with Lanthanum and Phosphorous. *Appl. Catal. A-General* **2012**, *417*, 137–144. https://doi.org/10.1016/j.apcata.2011.12.034.

(23) Martins, A.; Silva, J. M.; Ribeiro, M. F. Influence of Rare Earth Elements on the Acid and Metal Sites of Pt/HBEA Catalyst for Short Chain n-Alkane Hydroisomerization. *Appl. Catal. A-General* **2013**, *466*, 293–299. https://doi.org/10.1016/j.apcata.2013.06.043.

(24) Sushkevich, V. L.; Ivanova, I. I. Ag-Promoted ZrBEA Zeolites Obtained by Post-Synthetic Modification for Conversion of Ethanol to Butadiene. *ChemSusChem* **2016**, *9* (16), 2216–2225. https://doi.org/10.1002/cssc.201600572.

(25) Yu, D. N.; Dai, W. L.; Wu, G. J.; Guan, N. J.; Li, L. D. Stabilizing Copper Species Using Zeolite for Ethanol Catalytic Dehydrogenation to Acetaldehyde. *Chinese J. Catal.* **2019**, *40* (9), 1375–1384. https://doi.org/10.1016/S1872-2067(19)63378-4.

(26) Qi, L.; Zhang, Y.; Conrad, M. A.; Russell, C. K.; Miller, J.; Bell, A. T. Ethanol Conversion to Butadiene over Isolated Zinc and Yttrium Sites Grafted onto Dealuminated Beta Zeolite. *J. Am. Chem. Soc.* **2020**, *142* (34), 14674–14687. https://doi.org/10.1021/jacs.0c06906.

(27) Lopez, J. S.; Dagle, R. A.; Dagle, V. L.; Smith, C.; Albrecht, K. O. Oligomerization of Ethanol-Derived Propene and Isobutene Mixtures to Transportation Fuels: Catalyst and Process Considerations. *Catal. Sci. Technol.* **2019**, *9* (5), 1117–1131. https://doi.org/10.1039/c8cy02297f.

Renewable C_{4+} olefins can be selectively produced from ethanol over bimetallic copper- and lanthanum-containing Beta zeolite catalysts.